

# The Electronic Structure of Post-Transition Metal Oxides

David J. Payne

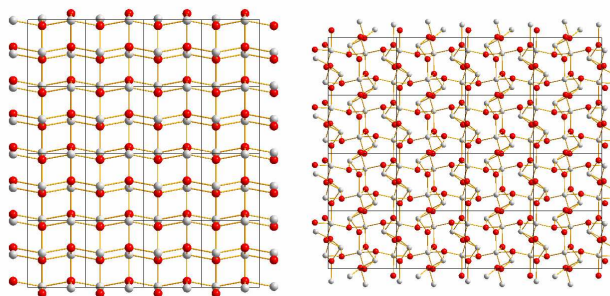
*Inorganic Chemistry Laboratory, University of Oxford, UK*

## Introduction

The global importance of post-transition metal oxides to a range of technologies are wide and far ranging, from  $\text{PbO}_2$  in the lead acid battery,<sup>1</sup> to  $\text{In}_2\text{O}_3$  and analogues in flat screen displays and solar panels.<sup>2</sup> The following work has attempted to further the understanding of the electronic structure of post-transition metal oxides, such as  $\text{PbO}$ ,<sup>3,4</sup>  $\text{PbO}_2$ ,<sup>4-8</sup>  $\text{Bi}_2\text{O}_3$ ,<sup>3,9</sup> and  $\text{In}_2\text{O}_3$ .<sup>10,11</sup> It is hoped that this work will provide new opportunities to exploit these valuable materials.

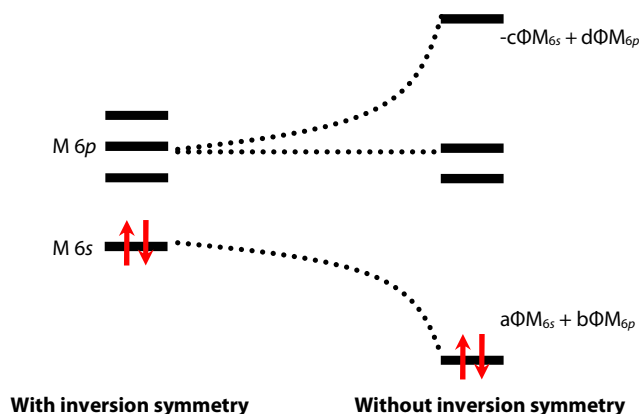
## A Revision of the Lone-Pair Model: $\text{PbO}$ and $\text{Bi}_2\text{O}_3$

Heavier post-transition elements such as Tl, Pb and Bi have two important oxidation states: the group state  $N$  and the  $N-2$  state. The crystal structures of  $N-2$  compounds frequently (but not always) involve irregular and non-centrosymmetric coordination environments for the metal cations: the oxides  $\alpha\text{-PbO}$  and  $\alpha\text{-Bi}_2\text{O}_3$  are typical in this respect.



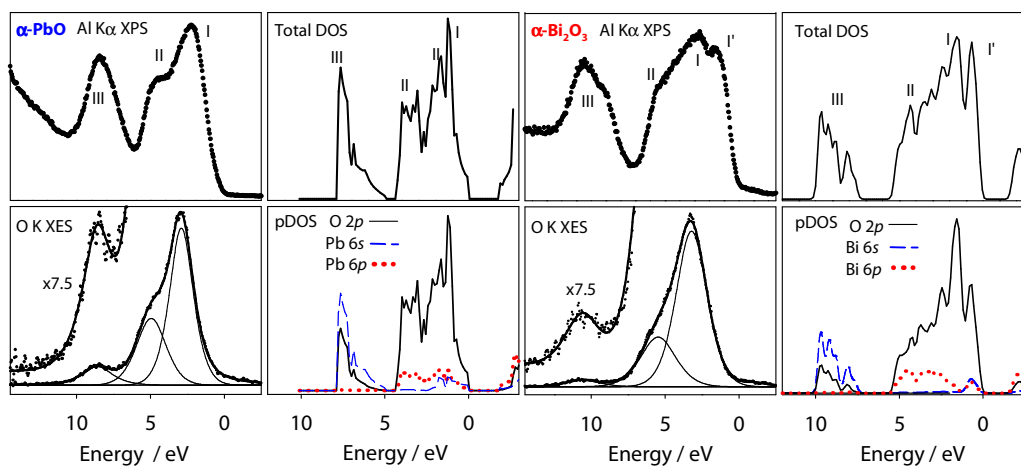
**Figure 9** The crystal structures of  $\alpha\text{-PbO}$  (left) and  $\alpha\text{-Bi}_2\text{O}_3$  (right). The oxygen atoms are red.

By simple electron counting the cations possess the  $6s^2$  electron configuration, and it is often assumed that the  $6s$  electrons must lie close to the Fermi energy ( $E_F$ ). Distorted structures are then rationalised in terms of a metal  $6s$ - $6p$  hybrid "lone-pair" orbital which is projected out into the void space within the distorted crystal structure, as shown in Figure 7.<sup>12</sup>



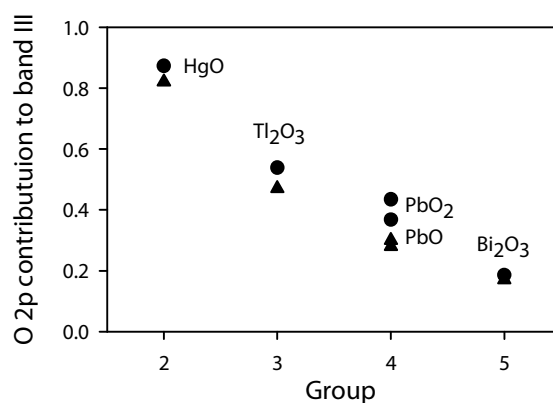
**Figure 7** Energy level diagram of the classical 'lone-pair' model.<sup>12</sup>

The conventional lone pair model has however recently been called into question on the basis of density functional calculations which suggest that the majority of the  $6s$  population in  $\alpha\text{-PbO}$  is in fact found at the bottom of the main valence band, about 10 eV below  $E_F$ .<sup>13</sup> Until now, no experimental evidence existed to support the theory.



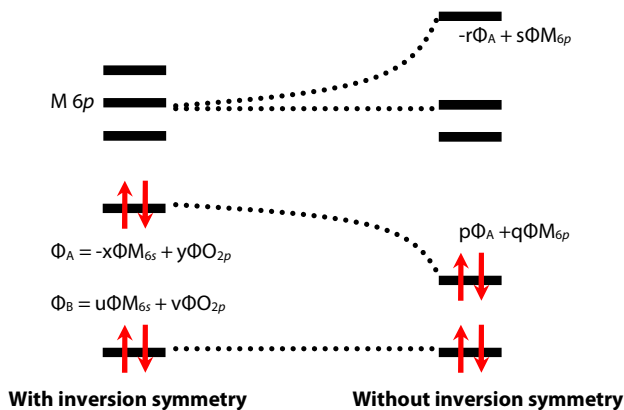
**Figure 8** Valence band Al K $\alpha$  XPS and O K shell XES spectra for  $\alpha$ -PbO (left four panels), and  $\alpha$ -Bi $_2$ O $_3$  (right four panels), compared with the total DOS and the pDOS derived from DFT bandstructure calculations.

O K shell emission spectra, directly measures the O 2p pDOS of the two oxides, and are shown in panels (a) and (g) of Figure 8. The weak intensity of band III is a clear signature of the fact that the corresponding electronic states at the bottom of the valence band have less O 2p character than the states closer to  $E_F$ , and are thereby are of dominant 6s character.



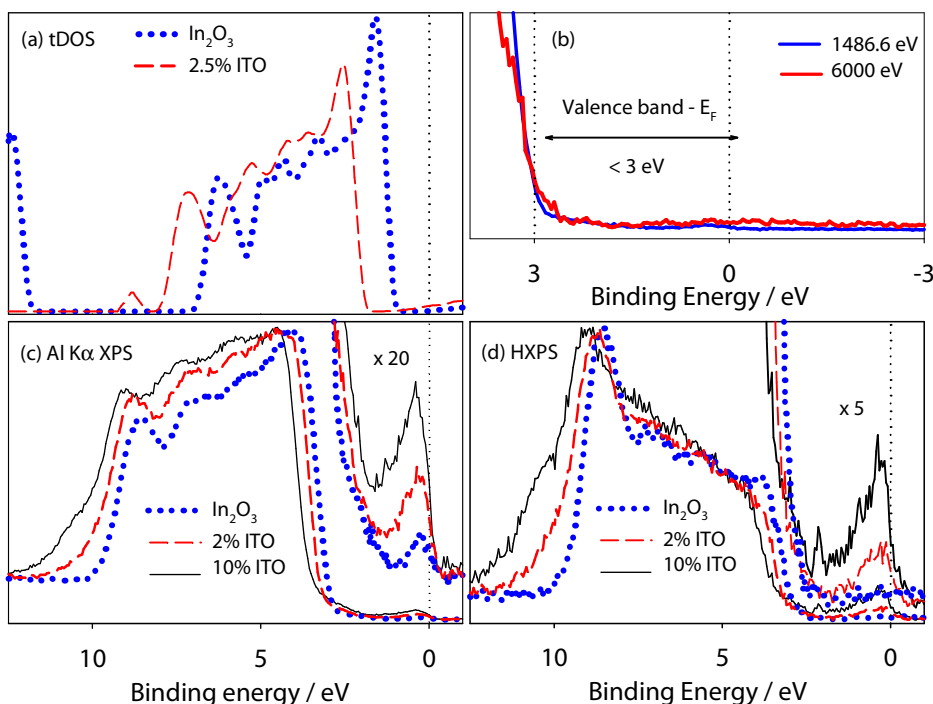
**Figure 8** Closed circles: estimated O 2p contribution to the lowest valence band state derived from intensities in O K shell XES spectra of the post-transition metal oxides HgO, Tl $_2$ O $_3$ , PbO $_2$ , PbO and Bi $_2$ O $_3$  as a function of group number.<sup>3</sup>

The results show that the the structural distortions found for  $\alpha$ -PbO and  $\alpha$ -Bi $_2$ O $_3$  *should not be attributed to direct mixing between cation levels close to the Fermi energy to give purely metal-based 6s-6p lone pairs*. The dominant contribution to the metal 6s PDOS is found at the bottom rather than the top of the valence band and indirect mixing between 6s and 6p states is mediated by hybridization with O 2p states at the top of the valence band.


**Figure 9** Energy level diagram of the revised 'lone-pair' model<sup>3</sup>

### The Electronic Structure of $\text{In}_2\text{O}_3$

Oxides that exhibit optical transparency *and* high conductivity, play a vital role in many, electronic devices. Prerequisites for oxides to display this phenomenon are; a bandgap larger than the visible light wavelength cut-off ( $\sim 410\text{nm}$ ), along with the presence of free charge carriers. The most important TCO is  $\text{In}_2\text{O}_3$  and the tin-doped analogue  $\text{Sn}_x\text{In}_{2-x}\text{O}_3$  (ITO). Surprisingly, there has been controversy of the magnitude of the band gap. The ubiquitously quoted value is  $3.75\text{ eV}$ .<sup>2</sup> However results from 1966 suggest an indirect bandgap of  $2.67\text{ eV}$ .<sup>14</sup>


**Figure 3** (a) Total density of states. (b) Valence band edges of  $\text{In}_2\text{O}_3$  measured using  $1486.6\text{ eV}$  and  $6000\text{ eV}$  photon energies. (c) Al K $\alpha$  ( $h\nu = 1486.6\text{ eV}$ ) XPS spectra. (d) HXPS ( $h\nu = 6000\text{ eV}$ ) spectra.

The valence band onset energy of  $2.9\text{ eV}$  for  $\text{In}_2\text{O}_3$  sets an *upper limit* for the fundamental bandgap. To help to understand these findings, electronic structure calculations of  $\text{In}_2\text{O}_3$  were performed.<sup>15</sup> The valence band maximum (VBM) state at  $\Gamma$  is threefold degenerate and is derived from O  $2p$  and In  $4d$  orbitals ( $\Gamma_4, T_g$  symmetry), while the conduction band minimum (CBM) state is a mixture of In  $5s$  and O  $2s$  orbitals ( $\Gamma_1, A_g$  symmetry). As the  $\text{In}_2\text{O}_3$  crystal structure contains an

inversion centre and the electric-dipole operator is of odd parity, *strong optical transitions are only permitted between two states of opposing parity*. These symmetry requirements result in a zero optical transition matrix element for direct VBM to CBM absorption at  $\Gamma$ , confirming that this  $\Gamma_4-\Gamma_1$  transition is formally forbidden. It is only from 0.81 eV *below* the VBM that strong transitions are observed. Here, the wavefunction character at  $\Gamma$  becomes sufficiently cation *p* like ( $\Gamma_8, T_u$  symmetry) and strong allowed optical transitions ( $5p \rightarrow 5s$ ) can occur.<sup>10, 11</sup>

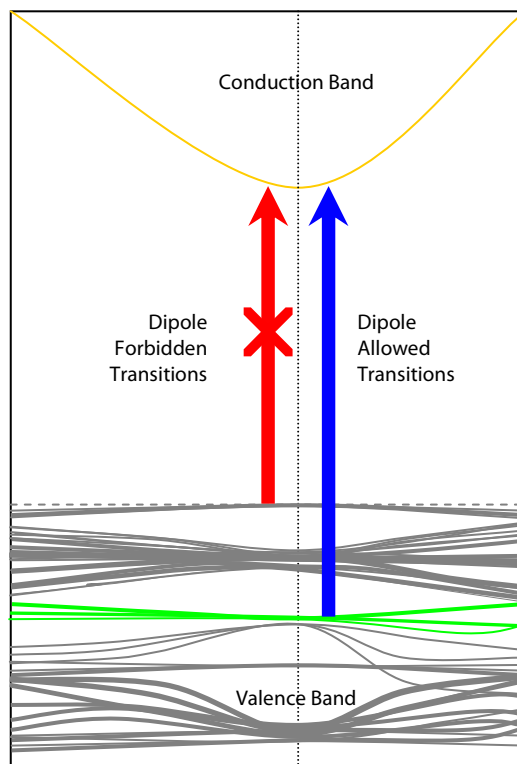


**Figure 5** Representation of the band structure of  $\text{In}_2\text{O}_3$ . The highest energy valence bands resulting in strong optical absorption to the conduction band are coloured green.

### The Electronic Structure of $\text{PbO}_2$

The importance of lead dioxide ( $\text{PbO}_2$ ) is often overlooked although it plays a critical role in the lead-acid battery. The reason for metallic behaviour of  $\text{PbO}_2$  is of crucial importance to the technological application of this material. A question often asked, but left unanswered is; why is lead dioxide metallic?

The results in Figure 6 show that the metallic nature observed in  $\text{PbO}_2$  is due to a partially filled conduction band that lies *above* the main valence band edge. These occupied states of strongly hybridised O  $2p$  and Pb  $6s$  orbitals, would be empty in stoichiometric  $\text{PbO}_2$ , and therefore an insulator. At 7700 eV, the partially filled conduction band appears as a well-defined peak. Occupation of the conduction band arises from electron induced donor states such as oxygen vacancy defects or proton interstitials. The observation that the carrier concentration increases after gentle annealing in UHV favours this vacancy hypothesis. These experiments give a value for the band gap of 0.61 eV.

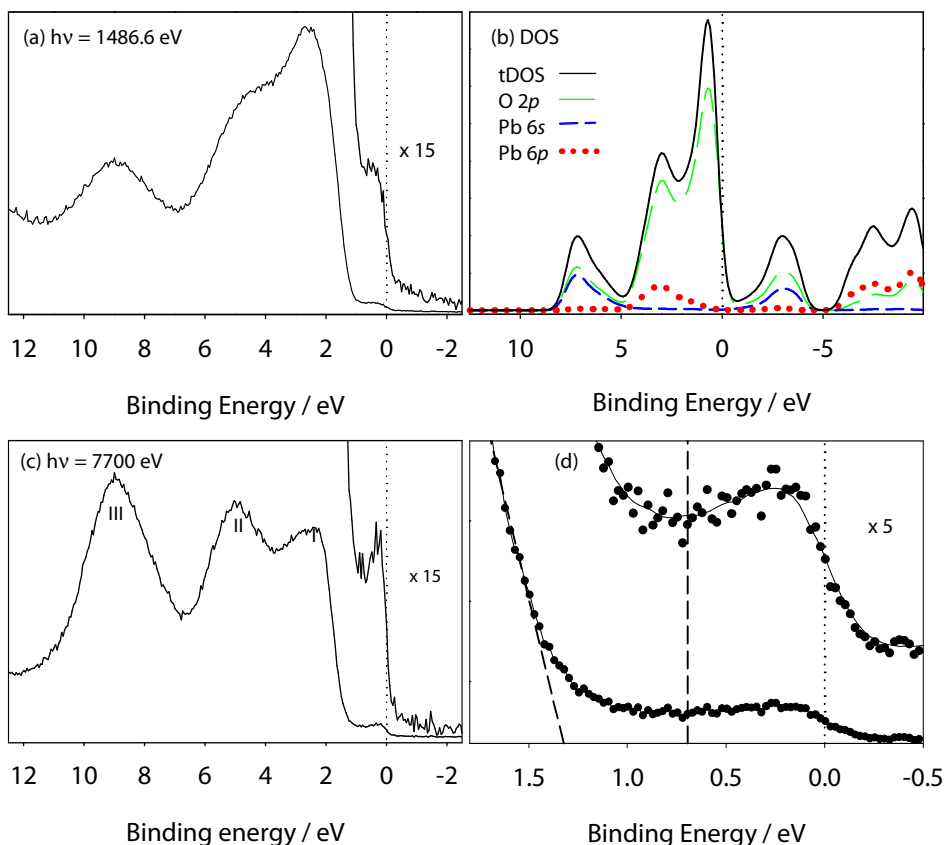


**Figure 1** (a) X-ray photoemission spectrum of PbO<sub>2</sub> measured at 1486.6 eV (b) Total density of states (tDOS) and partial density of states (pDOS). (c) HXPS of valence band measured at 7700 eV (d) HXPS of conduction band measured at 7700 eV.

**Conclusions**

The crystal structure of a material is critically dependent on its electronic structure, and it'ss this symbiotic relationship that determines the magnitude of band gap observed. Below is a periodic table which documents all known band gaps for 'group oxidation state' oxides. Included (in blue) are the two *new* values of band gaps for technologically important materials. It is hoped that this work will provide a valuable contribution to our understanding of the electronic structure of these diverse and important materials.

1	2	3	4	5	6	7	8	9	10	11	12	13	14	15	16	17	18
H <sub>2</sub> O ~9.0																	He
Li <sub>2</sub> O 8.0	BeO 10.6											B <sub>2</sub> O <sub>3</sub> 9.1	CO <sub>2</sub> ~12	N	O	F	N
Na <sub>2</sub> O ?	MgO 7.8											Al <sub>2</sub> O <sub>3</sub> 8.8	SiO <sub>2</sub> 8.9	P <sub>2</sub> O <sub>5</sub> ?	SO <sub>3</sub> ?	Cl <sub>2</sub> O <sub>7</sub> ?	Ar
K <sub>2</sub> O ?	CaO 7.1	Sc <sub>2</sub> O <sub>3</sub> 6.0	TiO <sub>2</sub> 3.1	V <sub>2</sub> O <sub>5</sub> 2.35	CrO <sub>3</sub> ?	Mn	Fe	Co	Ni	Cu	ZnO 3.4	Ga <sub>2</sub> O <sub>3</sub> 4.8	GeO <sub>2</sub> 4.63	As <sub>2</sub> O <sub>5</sub> ?	SeO <sub>3</sub> ?	Br	Kr
Rb <sub>2</sub> O ?	SrO 5.9	Y <sub>2</sub> O <sub>3</sub> 6.0	ZrO <sub>2</sub> 5.8	Nb <sub>2</sub> O <sub>5</sub> 3.9	MoO <sub>3</sub> 3.2	Tc <sub>2</sub> O <sub>7</sub> ?	Ru	Rh	Pd	Ag	CdO 0.55	In <sub>2</sub> O <sub>3</sub> 2.67	SnO <sub>2</sub> 3.6	Sb <sub>2</sub> O <sub>5</sub> ?	TeO <sub>3</sub> ?	I	XeO <sub>4</sub> ?
Cs <sub>2</sub> O ?	BaO 4.1	La <sub>2</sub> O <sub>3</sub> 6.0	HfO <sub>2</sub> 5.9	Ta <sub>2</sub> O <sub>5</sub> 4.4	WO <sub>3</sub> 2.6	Re <sub>2</sub> O <sub>7</sub> ?	OsO <sub>4</sub> ?	Ir	Pt	Au	HgO 1.9	Tl <sub>2</sub> O <sub>3</sub> 1.6	PbO <sub>2</sub> 0.61	Bi <sub>2</sub> O <sub>5</sub> ?	Po	At	Rn

A 'Group' oxidation state oxide  
 An element of the periodic table that does not achieve the 'Group' oxidation state in its oxides  
 A 'Group oxidation state' oxide that has had the band gap revised from work in this thesis

**Table 2** The periodic table of band gaps for the metal oxides that have attained 'group' oxidation state.<sup>16</sup>

**References** (Publications in blue contributed directly to the thesis)

1. R.M. Dell and D.A.J. Rand, *Understanding Batteries* (Royal Society of Chemistry, Cambridge, 2001).
2. I. Hamberg and C.G. Granqvist, *J. Appl. Phys.* **60** (1986) R123.
3. D.J. Payne, R.G. Egdell, A. Walsh, G.W. Watson, J. Guo, P.A. Glans, T. Learmonth, and K.E. Smith, *Phys. Rev. Lett.* **96** (2006) 157403.
4. D.J. Payne, R.G. Egdell, D.S.L. Law, P.A. Glans, T. Learmonth, K.E. Smith, J.H. Guo, A. Walsh, and G.W. Watson, *J. Mater. Chem.* **17** (2007) 267.
5. D.J. Payne, R.G. Egdell, W. Hao, J.S. Foord, A. Walsh, and G.W. Watson, *Chem. Phys. Lett.* **411** (2005) 181.
6. D.J. Payne, J.P. Hu, R.G. Egdell, V.R. Dhanak, and G. Miller, *Chem. Phys. Lett* **443** (2007) 61.
7. D.J. Payne, G. Paolicelli, F. Offi, G. Panaccione, P. Lacovig, G. Beamson, A. Fondacaro, G. Monaco, G. Vanko, and R.G. Egdell, *J. Electron. Spectrosc. Relat. Phenom.* **169** (2009) 26.
8. S. Rothenberg, D.J. Payne, A. Bourlange, and R.G. Egdell, *submitted to Journal of Materials Chemistry* (2007).
9. A. Walsh, G.W. Watson, D.J. Payne, R.G. Egdell, J. Guo, P.A. Glans, T. Learmonth, and K.E. Smith, *Phys. Rev. B* **73** (2006) 235104.
10. A. Walsh, J.L.F. Da Silva, S.-H. Wei, C. Körber, A. Klein, L.F.J. Piper, A. DeMasi, K.E. Smith, G. Panaccione, P. Torelli, D.J. Payne, A. Bourlange, and R.G. Egdell, *Phys. Rev. Lett.* **100** (2008) 167402.
11. A. Bourlange, D.J. Payne, R.G. Egdell, J.S. Foord, P.P. Edwards, M.O. Jones, A. Schertel, P.J. Dobson, and J.L. Hutchinson, *Appl. Phys. Lett.* **92** (2008) 092117.
12. L.E. Orgel, *J. Chem. Soc.* (1959) 3815.
13. G.W. Watson and S.C. Parker, *J. Phys. Chem. B* **103** (1999) 1258.
14. R.L. Weiher and R.P. Ley, *J. Appl. Phys.* **37** (1966) 299.
15. *Density Functional Theory (DFT) calculations were performed by Prof. Graeme Watson (Trinity College, Dublin) and Dr. Aron Walsh (Trinity College, Dublin and the National Renewable Energy Laboratory, Golden, Colorado).*
16. D.J. Payne, *The Electronic Structure of Post-Transition Metal Oxides*, D. Phil. Thesis, University of Oxford (2008).